GMR
The Original

FABRICATION OF BIOCOMPATIBLE STARCH/PVA/CuO ELECTROSPUN NANOSCAFFOLDS FROM MARINE MACROALGAE (*Gracilaria corticata*) EXTRACT FOR ENHANCED ANTI-INFLAMMATORY ACTIVITY

Aksitha Sakthiraj[1], Darshini Adhinathan[2], Abyramy Balasundaram[2], Alagendran Subbarayalu[3]*

[1]Saveetha Medical College & Hospital (SMCH), Saveetha Institute of Medical and Technical Sciences (SIMATS), Thandalam, Chennai, Tamil Nadu 602105, India. aksitha2004sakthiraj@gmail.com
[2]Department of Dermatology, Saveetha Medical College and Hospital, Saveetha Institute of Medical And Technical Sciences (SIMATS), Thandalam, Chennai-602105, Tamil Nadu, India. Email: darshiniadhinathan1998@gmail.com; b.abyramy@gmail.com.
[3]Clinical Neuroscience and Phytomedicine Laboratory, Department of Research, Saveetha College of Nursing (SCON), Saveetha Institute of Medical and Technical Sciences (SIMATS), Chennai 602105, Tamil Nadu, India. Email: proteinblg@gmail.com; alagendrans.scon@saveetha.com. ORCID: https://orcid.org/0009-0009-0749-7180.
*Correspondence: proteinblg@gmail.com; alagendrans.scon@saveetha.com (A.S.)

ABSTRACT
This study reports the fabrication and evaluation of biocompatible electrospun nanoscaffolds composed of starch and polyvinyl alcohol (PVA) incorporated with copper oxide (CuO) nanoparticles synthesized via an ultrasonic-assisted green method using *Gracilaria corticata* extract. UV–Vis analysis confirmed the formation of CuO NPs through surface plasmon resonance at 291 nm, while Fourier-transform infrared spectroscopy (FTIR) and X-ray diffraction (XRD) validated the successful integration and crystallinity of nanoparticles within the polymer matrix. scanning electron microscopy (SEM) images revealed smooth, bead-free nanofibers with well-dispersed CuO NPs, and thermogravimetric analysis (TGA) demonstrated improved thermal stability. Dynamic light scattering (DLS) and zeta potential studies showed moderate stability and nanoscale size distribution. The developed nanoscaffolds exhibited significant anti-inflammatory activity in protein denaturation and xanthine oxidase inhibition assays, outperforming both the algal extract and nanoparticles alone. These results highlight the synergistic effect of the polymer-nanoparticle composite and its potential for biomedical applications. The study underscores the value of marine-derived phytochemicals in the eco-friendly synthesis of functional nanomaterials for therapeutic use.

KEYWORDS: *Gracilaria corticata*, Green synthesis, CuO nanoparticles, starch/PVA/CuO-NPs nanoscaffolds, Anti-inflammatory activity.

1. INTRODUCTION

In recent years, the confluence of nanotechnology and green chemistry has catalyzed the development of multifunctional biomaterials with promising applications in the fields of biomedicine, drug delivery, wound healing, and tissue engineering [1]. A major focus in this domain is the design of nanostructured scaffolds that mimic the natural extracellular matrix (ECM) while incorporating bioactive agents to confer additional therapeutic benefits such as antimicrobial, antioxidant, or anti-inflammatory properties [2]. Among the various nanostructures explored, electrospun nanofibrous scaffolds have emerged as highly versatile systems due to their large surface area-to-volume ratio, tunable porosity, and excellent physical resemblance to ECM, making them particularly suitable for biomedical applications [3].

The use of naturally derived polymers in scaffold fabrication has gained considerable attention due to their intrinsic biocompatibility, biodegradability, and minimal cytotoxicity [4]. Starch, a widely available and renewable polysaccharide, offers a cost-effective and biodegradable matrix for scaffold design [5]. However, native starch possesses limitations in terms of mechanical strength and processability, which necessitate blending with synthetic polymers [6]. Polyvinyl alcohol (PVA), a water-soluble, biocompatible synthetic polymer, is frequently used in combination with natural polymers to enhance mechanical properties and spinnability [7]. The starch/PVA blend, when electrospun into nanofibers, yields a robust, biocompatible, and biodegradable scaffold suitable for hosting therapeutic nanoparticles [8].

Copper oxide nanoparticles (CuO NPs) have attracted significant research interest for their diverse biological activities, including antimicrobial, anticancer, antioxidant, and anti-inflammatory properties [9]. CuO NPs possess

excellent physicochemical stability and redox properties, making them effective candidates for integration into polymeric biomaterials [10]. However, conventional synthesis routes for CuO NPs often involve hazardous chemicals, energy-intensive processes, and generate toxic byproducts, which limit their biomedical applicability [11]. To circumvent these drawbacks, the green synthesis approach has emerged as a sustainable and eco-friendly alternative [12]. In particular, marine macroalgae offer a rich repository of reducing and stabilizing agents such as polysaccharides, phenolics, flavonoids, and terpenoids, which can facilitate the bioreduction of metal ions to nanoparticles under mild reaction conditions [13].

Gracilaria corticata, a species of red marine macroalga abundant along the Indian coastline, particularly in regions like Rameswaram, has been recognized for its diverse bioactive profile [14]. Rich in sulfated polysaccharides, vitamins, minerals, and phenolic compounds, *G. corticata* serves as an ideal bioresource for the green synthesis of metal nanoparticles [15]. In this study, ultrasonic-assisted extraction (UAE) was employed to enhance the release of these bioactives, which subsequently facilitated the bioreduction of copper salts into CuO NPs [16]. UAE is a non-thermal, efficient, and scalable extraction method that enhances cell wall disruption, accelerates mass transfer, and preserves thermolabile compounds, making it highly suitable for extracting bioactives from macroalgal biomass [17].

Integrating green-synthesized CuO NPs into starch/PVA electrospun nanoscaffolds offers a multifunctional biomaterial platform with both structural and therapeutic capabilities [18]. The incorporation of CuO NPs within the nanofibrous matrix not only enhances the scaffold's mechanical integrity and thermal stability but also imparts bioactivity, particularly anti-inflammatory effects [19]. Chronic inflammation underlies a wide range of pathological conditions, including autoimmune diseases, cardiovascular disorders, and chronic wounds [20]. Therefore, developing scaffolds with intrinsic anti-inflammatory potential is of great interest for regenerative medicine and wound care [21].

To evaluate the therapeutic potential of the developed nanoscaffold, two complementary *in vitro* assays were employed: the protein denaturation inhibition assay and the xanthine oxidase inhibition assay [22]. The former assesses the scaffold's capacity to prevent protein aggregation, a common marker of inflammation, while the latter evaluates its ability to inhibit xanthine oxidase activity, a key enzyme in reactive oxygen species (ROS) generation and uric acid production [23]. Together, these assays provide a comprehensive assessment of the scaffold's anti-inflammatory efficacy.

In addition to biological evaluation, extensive physicochemical characterization of the CuO NPs and nanofibrous scaffolds was performed using a range of analytical tools [24]. UV-Visible spectroscopy, Fourier-transform infrared spectroscopy (FTIR), and X-ray diffraction (XRD) confirmed the formation and structural integration of CuO NPs, while scanning electron microscopy (SEM) analysis provided insights into fiber morphology and nanoparticle dispersion [25]. Dynamic light scattering (DLS) and zeta potential measurements established nanoparticle size and colloidal stability, critical factors for *in vivo* applications [26]. Thermogravimetric analysis (TGA) further demonstrated the enhanced thermal resilience of the CuO-incorporated scaffolds [27].

This research presents a comprehensive strategy combining green nanotechnology, marine bioresources, and advanced fabrication techniques to create a novel nanoscaffold with dual structural and therapeutic roles [28]. The novelty of this work lies in the synergistic use of starch/PVA polymer matrices, green-synthesized CuO NPs, and UAE from *G. corticata*, leading to a sustainable and biofunctional nanoscaffold [29]. The developed material holds promise for a range of biomedical applications, particularly in inflammation-associated conditions and regenerative therapies [30].

By integrating marine-based nanotechnology and electrospinning, this study advances the frontier of eco-friendly biomaterial development [28]. Furthermore, it aligns with global sustainability goals by utilizing abundant natural resources and minimizing the environmental footprint of nanomaterial synthesis [31]. Overall, the findings contribute to the growing body of research on green nanotechnology for biomedicine and open new avenues for the development of multifunctional, therapeutic scaffolds for future clinical applications.

2. MATERIALS AND METHODS

2.1 Chemicals and reagents

The brown seaweed *G. corticata* was harvested from the coastal waters of Rameswaram, Tamil Nadu, India, and used as a sustainable source for the eco-friendly synthesis of CuO NPs. Analytical-grade copper (II) sulfate pentahydrate ($CuSO_4 \cdot 5H_2O$), purchased from Merck, acted as the copper precursor. PVA with a molecular weight of approximately 115,000 g/mol, along with starch, was utilized to fabricate biocompatible, biodegradable nanofibrous scaffolds. Electrospinning was carried out using a HOLMARC HO-NFES-040 unit. All additional solvents and reagents were acquired from Sigma-Aldrich and Merck, maintaining analytical-grade standards to ensure experimental consistency. The characterization of the synthesized CuO NPs and nanofibrous scaffolds

involved UV-Visible spectrophotometry, FTIR spectroscopy, XRD, SEM, DLS, zeta potential analysis, and TGA. Anti-inflammatory activity was assessed using standardized *in vitro* assays.

2.2 Collection and processing of marine algae

The brown macroalga *G. corticata* was collected from the intertidal zone along Rameswaram's coast. Post-harvest, samples were kept in chilled containers to retain bioactive integrity. The algal material was washed thoroughly with tap water to remove debris and epiphytes, followed by multiple rinses with distilled water to clear residual salts. Around 100 g of cleaned algae were cut into small pieces and air-dried for two weeks under ambient conditions. The dried biomass was then ground into a fine powder using a mechanical grinder and stored in airtight containers in a cool, dry place.

2.3 UAE of bioactive compounds

Bioactives were extracted from powdered *G. corticata* via UAE to enhance cell wall disruption and extract yield. A total of 2 g dried algal powder was suspended in 50 mL Milli-Q water in a 100 mL borosilicate beaker. This suspension underwent ultrasonication at 60°C for 45 minutes using a LABQUEST ultrasonic cleaner (Borosil; Serial No. 941032329018). The resulting extract was filtered through sterile Whatman No. 1 paper. The clear filtrate was refrigerated at 10°C and a portion was freeze-dried for use in CuO NP synthesis [32].

2.4 Green synthesis of CuO NPs

The biosynthesis of CuO NPs was carried out by combining algal extract with an aqueous copper salt solution. A 0.1 M $CuSO_4 \cdot 5H_2O$ solution (50 mL) was mixed with 10 mL of algal extract (10 mg/mL), maintaining a 5:1 ratio of precursor to extract. The mixture was stirred at 650 rpm and heated to 60°C for 2 hours on a magnetic stirrer with a hotplate. The color change from deep blue to bluish-green signified Cu^{2+} reduction by phytochemicals. The synthesized CuO NPs were washed thrice with double-distilled water and freeze-dried for 48 hours, yielding a fine powder for scaffold integration and bioassays [33].

2.5 Preparation of starch/PVA nanofibrous scaffolds loaded with CuO NPs

Nanofibrous scaffolds were fabricated using a starch-PVA blend incorporating the biosynthesized CuO NPs. A 15% (w/w) PVA solution was prepared by dissolving the polymer in Milli-Q water with continuous stirring at 50°C. Subsequently, 100 mg of starch and 100 mg of CuO NPs were added, and the mixture was stirred for 2.5 hours at 50°C to achieve uniform dispersion. The viscous solution was loaded into a 10 mL syringe with a stainless-steel needle (0.84 mm internal diameter). Electrospinning was conducted using the HOLMARC HO-NFES-040 setup under optimized conditions: 11.5 kV voltage, 12.3 cm tip-to-collector distance, and 0.4 mL/h flow rate. Electrospinning was carried out at ambient temperature over 6–8 hours. The resulting mats were collected and stored in desiccators to preserve their morphology [34, 35].

2.6 Physicochemical characterization

2.6.1 UV-visible spectroscopy

Absorption spectra of the algal extract, CuO NPs, and CuO-incorporated starch/PVA nanofibers were recorded with a VIS SPEC V-730 spectrophotometer over 200–800 nm, using deionized water as the reference. Absorption bands between 270–300 nm indicated surface plasmon resonance, confirming CuO NP formation [36].

2.6.2 FTIR spectroscopy

Functional group identification and interaction analysis were performed via FTIR using a PerkinElmer Spectrum Two instrument in ATR mode. Spectra were recorded between 4000–400 cm^{-1} at 4 cm^{-1} resolution with 64 scans/sample. Prominent peaks for hydroxyl (O–H), carbonyl (C=O), amide, and metal-oxygen (Cu–O) were observed, confirming nanoparticle integration [37, 38].

2.6.3 XRD analysis

XRD patterns of CuO NPs and scaffolds were acquired using a Bruker D8 Advance diffractometer with CuKα radiation (λ = 1.5406 Å), operated at 40 kV and 40 mA. Scans were conducted over a 2θ range of 5°–90° with a 0.029649° step. Sharp peaks consistent with monoclinic CuO phase confirmed crystallinity, and shifts in composite peaks indicated NP embedding [39].

2.6.4 SEM imaging

The scaffold morphology and nanoparticle dispersion were analyzed via SEM (JEOL JSM-IT800 NANO). Prior to imaging, samples were sputter-coated with gold. SEM images revealed uniform nanofibers with minimal bead formation and even CuO NP distribution [32].

2.6.5 TGA

TGA was performed using a PerkinElmer TGA 8000. Approximately 5 mg of sample was heated from room temperature to 550°C at 15°C/min under nitrogen. Mass loss curves identified phases of moisture loss, polymer breakdown, and composite degradation. CuO-containing scaffolds displayed enhanced thermal resistance [40].

2.6.6 DLS and zeta potential

Hydrodynamic size and zeta potential of CuO NPs were measured using a Malvern Zetasizer Ultra. DLS determined particle size and polydispersity index (PDI), while zeta potential values above ±30 mV indicated good colloidal stability and dispersion, relevant for biomedical applications [41].

All raw and processed data were made available via the Mendeley Data repository (DOI: 10.17632/763h4wwkrj.2) for reproducibility and transparency.

2.7 Anti-inflammatory evaluation

2.7.1 Protein denaturation inhibition assay

Anti-inflammatory activity was assessed using a modified heat-induced protein denaturation assay. Each 0.5 mL reaction mix included 0.45 mL of 5% bovine serum albumin and 0.05 mL of test sample (algal extract, CuO NPs, scaffold, or diclofenac sodium) at 25, 50, 75, and 100 µg/mL. After adjusting pH to 6.3 with 1 N HCl, mixtures were incubated at 37°C for 20 min, heated at 57°C for 3 min, and cooled. Absorbance at 660 nm indicated turbidity from protein denaturation [42].

2.7.2 Xanthine oxidase inhibition assay

Xanthine oxidase inhibition was evaluated using a modified protocol. Reaction mixtures consisted of 0.3 mL of sample (25–100 µg/mL), 0.5 mL of 0.15 mM xanthine (in phosphate buffer, pH 7.5), and 0.2 mL xanthine oxidase (0.1 units/mL). Samples were incubated at 25°C for 15 minutes. Absorbance at 295 nm measured uric acid formation. Enzyme-free blanks served as controls [43].

2.8 Statistical analysis

All experimental results were analyzed using SPSS v25.0 and GraphPad Prism v9.0. Triplicate assays were conducted, and results were reported as mean ± standard deviation. One-way ANOVA followed by Tukey's or Dunnett's post-hoc test determined significance ($p < 0.05$). Shapiro-Wilk test assessed data normality, and log transformation was applied when needed. Pearson correlation coefficients assessed inter-variable relationships. All statistical conclusions were drawn at a 95% confidence level [44].

3. RESULTS

3.1. UV–visible spectroscopy

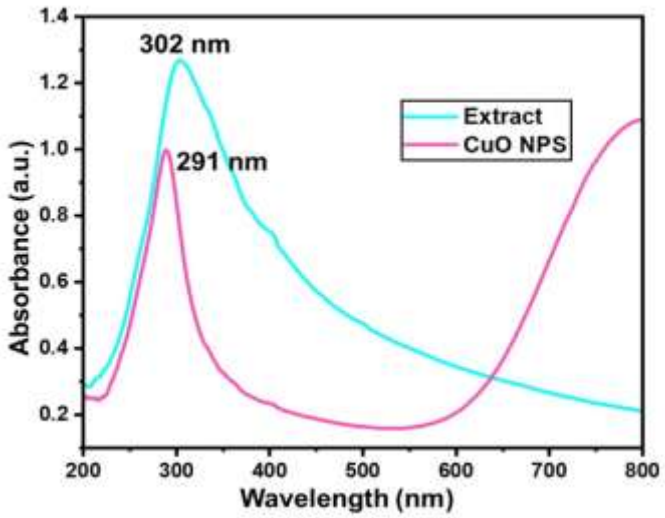

Fig. 1. UV–Visible spectral profiles of algal extract and CuO nanoparticles.

The UV–Visible spectral analysis (Fig. 1) shed light on the optical properties of both the *G. corticata* extract and the green-synthesized CuO NPs. The aqueous extract displayed a broad absorption profile ranging between 800

nm and 200 nm, with the highest absorbance value recorded at 302 nm (1.268). This extensive absorbance is typical of phytoconstituents such as polyphenols and flavonoids, which facilitate the reduction and stabilization of metal ions during nanoparticle synthesis. In contrast, the CuO NPs presented a sharp surface plasmon resonance (SPR) peak at 291 nm, a signature of nanoparticle formation arising from conduction band electron oscillations. Additionally, the CuO NPs showed significant absorbance at higher wavelengths (1.200 at 800 nm), which decreased steadily toward shorter wavelengths, consistent with metal oxide nanoparticles. The extract's lack of distinct peaks and the emergence of a clear SPR band in the nanoparticle sample confirm the biosynthesis of CuO NPs using the *G. corticata* extract as a reducing and stabilizing agent.

3.2. FTIR spectroscopy analysis

FTIR spectra (Fig. 2), recorded in ATR mode using a PerkinElmer Spectrum Two spectrometer, were used to identify functional groups in the CuO NPs and the nanoscaffold composite. The CuO NPs spectrum exhibited bands related to O–H stretching and Cu–O vibrations, validating metal-oxygen bond formation. The nanoscaffold displayed ten significant peaks: a broad O–H stretch at 3303.50 cm^{-1}, a C=O stretch at 1709.35 cm^{-1}, aliphatic C–H stretching at 2924.80 cm^{-1}, and additional peaks at 1427.14, 1329.09, 1141.87, 1088.65, 919.75, 843.06, and 601.37 cm^{-1}, indicative of polymeric components such as amides and polysaccharides. These spectral features confirm CuO NPs' integration into the polymer matrix and their interaction with functional groups, likely through metal coordination and hydrogen bonding. The detection of plant-derived bioactive groups suggests that *G. corticata* extract plays a stabilizing role at the nanoparticle interface.

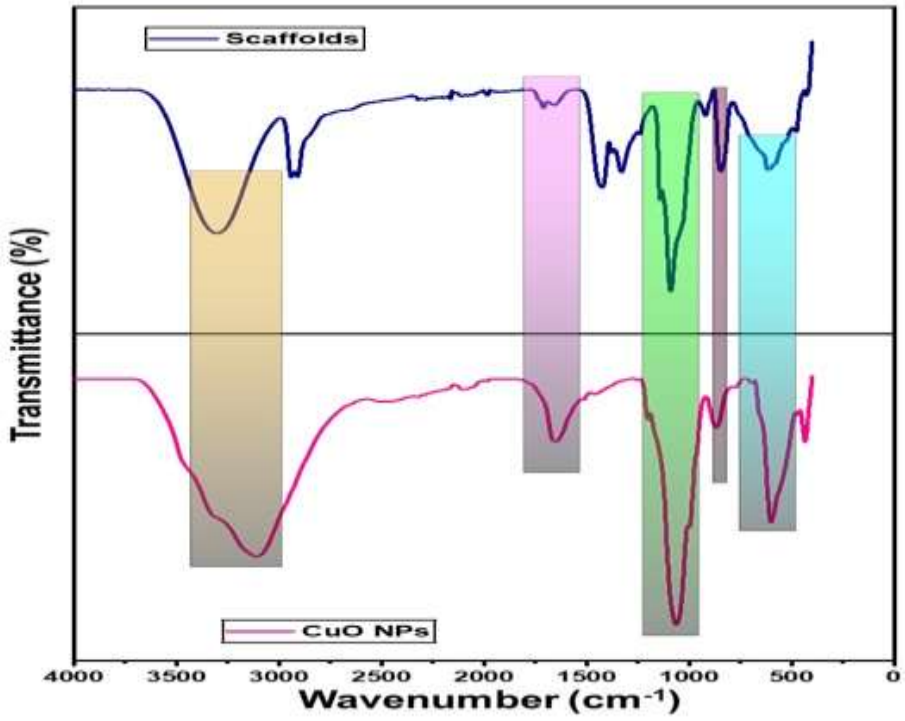

Fig. 2. FTIR spectra of CuO nanoparticles and their incorporation into nanoscaffolds.

3.3. XRD analysis

XRD analysis, performed using a Bruker D8 Advance diffractometer, revealed the crystallographic properties of the synthesized CuO NPs and the nanoscaffold composite. The CuO NPs showed 37 peaks within a 2θ range of 12.852° to 57.284°, with strong diffraction at 19.134°, 24.369°, and 15.797°, consistent with monoclinic CuO (JCPDS 48-1548). These peaks corresponded to d-spacings of 4.63468 Å, 3.64963 Å, and 5.60549 Å, confirming their crystalline and pure nature. The nanoscaffold displayed 13 diffraction peaks, notably at 29.445° and 21.346°, suggesting a semi-crystalline structure with 20.2% crystalline and 79.8% amorphous content. Broadened peaks, such as the one at 43.067° with a FWHM of 1.025°, indicated smaller crystallite size and good integration of CuO NPs into the matrix. Slight peak shifts, like the shift from 35.999° to 36.034°, implied strong interfacial bonding between the nanoparticles and the polymer, possibly facilitated by stabilizing phytochemicals from *G. corticata* extract.

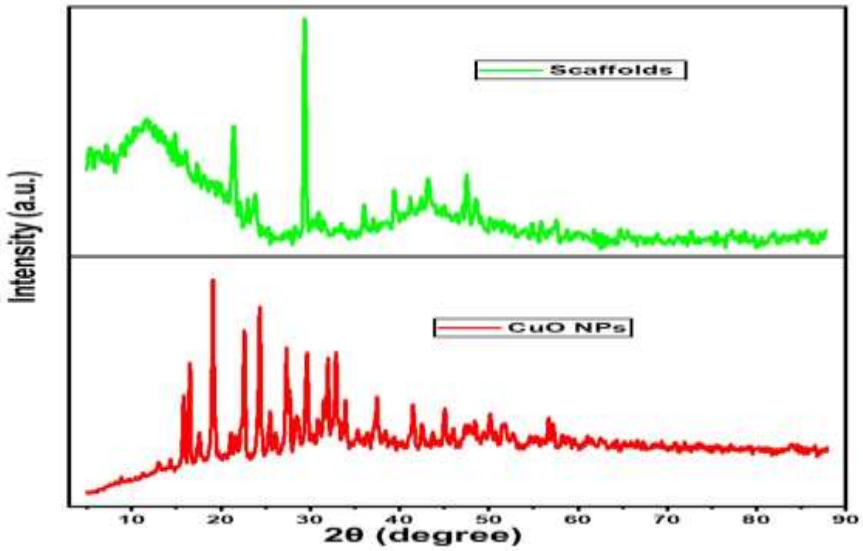

Fig. 3. XRD patterns of synthesized CuO nanoparticles and CuO-loaded scaffolds.

3.4. SEM analysis

The morphological and distributional characteristics of CuO NPs within electrospun starch/PVA nanoscaffolds were examined using a JEOL JSM-IT800 NANO SEM system. The images revealed a continuous fibrous network with smooth surfaces and fiber diameters between 90 and 150 nm. No bead formation or fiber damage was visible, indicating successful electrospinning. Spherical CuO NPs under 100 nm were uniformly dispersed on the nanofiber surfaces and embedded within the matrix without clustering. This even distribution confirms the effective blending of nanoparticles into the polymeric solution before electrospinning. The unaltered morphology affirms the compatibility of CuO NPs with the starch/PVA scaffold. The *G. corticata* extract played a critical role in maintaining nanoparticle dispersion and preventing agglomeration due to its natural capping agents.

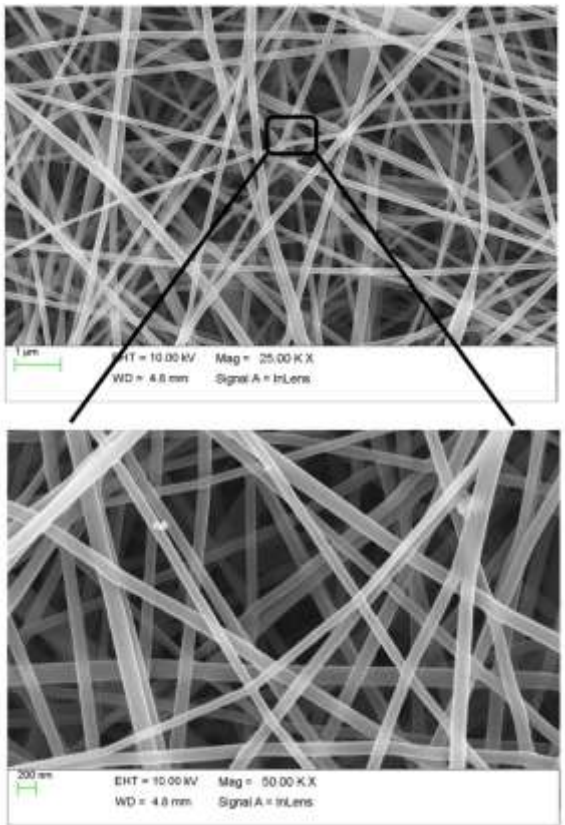

Fig. 4. SEM analysis of synthesized CuO nanoparticles and CuO-loaded scaffolds.

3.5. TGA

TGA of the nanoscaffold was carried out using a PerkinElmer thermal analyzer by heating the sample from 30°C to 550°C at 15°C/min. The thermogram displayed two main degradation stages: the first began at 265.25°C with a peak decomposition at 355.41°C, related to the breakdown of organic residues and polymers; the second started at 425.38°C, with maximum degradation at 448.38°C, corresponding to the degradation of more thermally stable components. Total weight loss was calculated at -33.372%, outlining the scaffold's thermal breakdown profile. The high initial decomposition temperatures indicate improved thermal resistance, likely due to CuO NP reinforcement and potential cross-linking. Additionally, secondary metabolites from *G. corticata* may enhance this thermal performance through protective interactions with polymer chains.

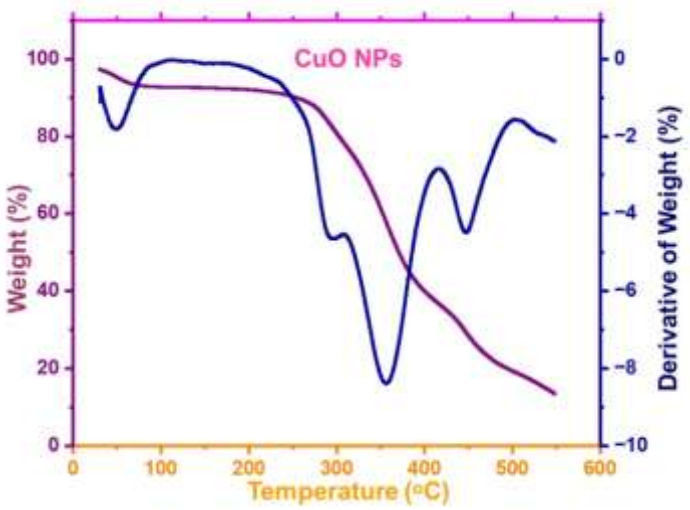

Fig. 5. Thermal degradation behavior of CuO-incorporated nanoscaffolds.

3.6. DLS and zeta potential analysis

DLS and zeta potential measurements were performed using a Malvern Zetasizer to evaluate the colloidal characteristics of the biosynthesized CuO NPs. The nanoparticles exhibited a bimodal size distribution with an average diameter (Z-average) of 68.6 nm and a PDI of 0.584, suggesting moderate heterogeneity in particle size. The zeta potential measured -14.11 mV, with peaks at -25.21 mV and -5.514 mV, indicating a moderately negative surface charge that supports partial colloidal stability. This charge can be attributed to negatively charged biomolecules from the *G. corticata* extract. The recorded conductivity was 0.05175 mS/cm, and the wall zeta potential was -12.73 mV. While these results show adequate dispersion stability, further surface modification may be required to enhance long-term colloidal behavior, particularly for biomedical applications requiring consistent nanoparticle performance.

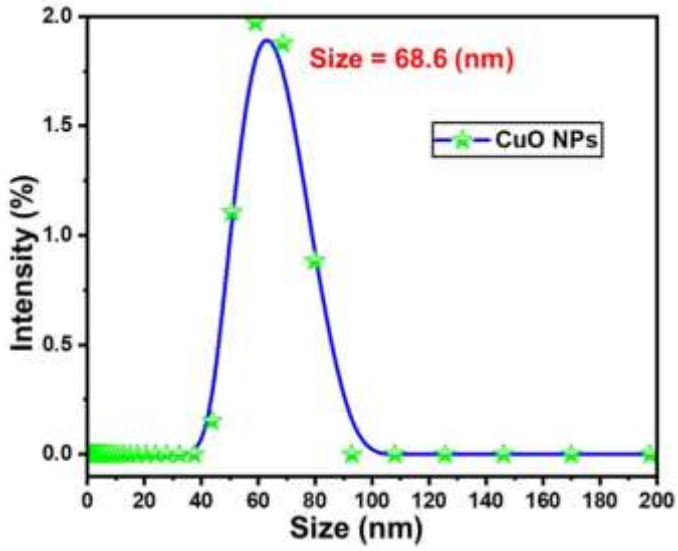

Fig.6. DLS particles size analysis of CuO NPs

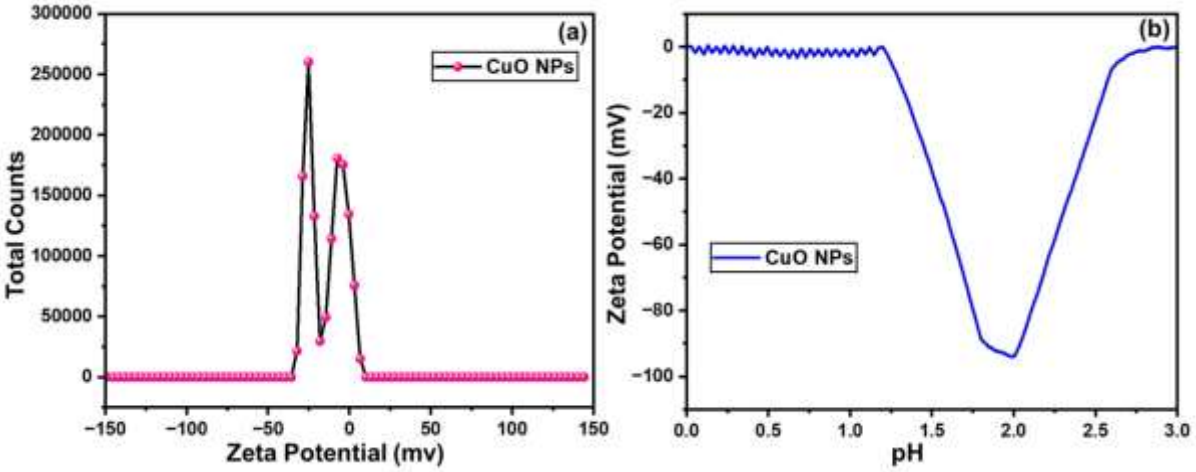

Fig.7. Zeta-potential analysis of CuO NPs

3.7. Anti-inflammatory assays

3.7.1. Protein denaturation inhibition assay

The protein denaturation inhibition assay evaluated the anti-inflammatory potential of algal extract, CuO NPs, and starch/PVA/CuO-NPs nanoscaffolds by measuring their ability to prevent heat-induced denaturation of bovine serum albumin (BSA). The results demonstrated concentration-dependent inhibition across all samples. At 25 µg/mL, the algal extract exhibited 20.95% inhibition, while CuO NPs and nanoscaffolds showed higher efficacy at 24.95% and 27.95%, respectively. As the concentration increased to 100 µg/mL, the inhibition rates rose significantly, with the extract reaching 65.15%, CuO NPs 71.15%, and nanoscaffolds 81.15%. Notably, the nanoscaffolds outperformed both the extract and CuO NPs at all concentrations, suggesting enhanced stabilization of protein structures, likely due to the synergistic effects of the polymer matrix and nanoparticles.

In a replicate experiment, similar trends were observed, though slight variations in inhibition percentages were noted. For instance, at 100 µg/mL, the extract, CuO NPs, and nanoscaffolds achieved 65.14%, 72.14%, and 79.14% inhibition, respectively. These results confirm the reproducibility of the assay and underscore the superior anti-inflammatory activity of the nanoscaffolds, which approached the efficacy of the standard drug (diclofenac sodium) at higher concentrations.

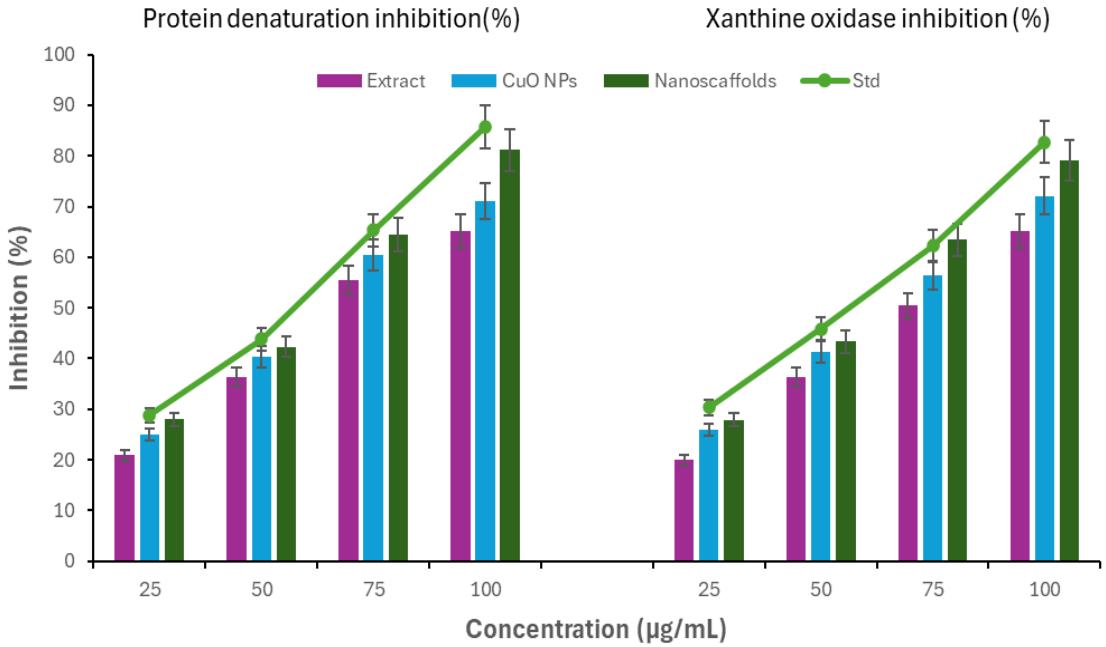

Fig.8. Anti-inflammatory activity analysis of algal extract, CuNPs and starch/PVA/CuONPs nanoscaffolds

3.7.2. Xanthine oxidase inhibition assay

The xanthine oxidase inhibition assay assessed the ability of the test samples to suppress uric acid production, a key marker of inflammation. The algal extract displayed moderate inhibition, with values ranging from 19.94% at 25 µg/mL to 65.14% at 100 µg/mL. CuO NPs exhibited stronger inhibitory effects, increasing from 25.94% to 72.14% over the same concentration range. The nanoscaffolds consistently demonstrated the highest inhibition, reaching 79.14% at 100 µg/mL, indicative of their potent xanthine oxidase inhibitory activity.

The replicate data further validated these findings, with minor deviations likely attributable to experimental variability. For example, at 75 µg/mL, the nanoscaffolds achieved 63.46% inhibition in the second trial, compared to 64.48% in the first, highlighting their robust performance. The superior efficacy of the nanoscaffolds may stem from their composite structure, which enhances bioavailability and interaction with the enzyme.

Both assays revealed that the starch/PVA/CuO-NPs nanoscaffolds exhibited the highest anti-inflammatory activity, followed by CuO NPs and the algal extract. The nanoscaffolds' performance suggests their potential as a promising alternative to conventional anti-inflammatory agents, combining the benefits of natural extracts and nanotechnology. Further studies could explore their mechanisms of action and *in vivo* efficacy to validate these findings.

4. DISCUSSION

The present study comprehensively elucidates the successful green synthesis of copper oxide CuO NPs using *G. corticata* extract and their subsequent incorporation into starch/PVA nanofibrous scaffolds. Each characterization technique provided critical insight into the physicochemical properties, structural morphology, and bioactivity of the resulting nanomaterials.

The UV–Visible spectroscopy results underscore the distinct optical properties of the algal extract and the CuO NPs. The broad absorption range exhibited by the extract, especially the intense peak at 302 nm, is consistent with the presence of phenolic and flavonoid compounds, which are known to participate in redox reactions facilitating the reduction of metal ions. These phytochemicals serve dual functions as both reducing and capping agents. The shift in the spectral profile for the synthesized CuO NPs, particularly the sharp absorption at 291 nm, signifies the formation of nanoparticles and the establishment of a surface plasmon resonance (SPR), characteristic of CuO. This SPR peak, coupled with the declining absorbance from 800 nm to 200 nm, aligns with the known optical features of metal oxide nanoparticles. The contrast in spectral profiles between the extract and the CuO NPs provides strong evidence of successful biosynthesis and indicates the role of plant-derived metabolites in stabilizing the nanostructures [45-49].

FTIR spectroscopy provided deeper insights into the functional groups involved in nanoparticle stabilization and scaffold formation. For the CuO NPs, typical peaks associated with O–H stretching and Cu–O bending confirmed the formation of metal-oxygen bonds. The starch/PVA/CuO nanoscaffold exhibited a more complex spectral profile with characteristic peaks corresponding to hydroxyl, carbonyl, and aliphatic hydrocarbon groups. Additionally, prominent signals at 1427.14 cm^{-1} and 1329.09 cm^{-1} likely stem from amide bonds and polysaccharide backbones. These findings suggest strong intermolecular interactions, including hydrogen bonding and possible chelation between CuO and the polymeric matrix. The preservation of bioactive functional groups from the algal extract indicates their role in facilitating the compatibility between inorganic nanoparticles and organic scaffolds [50-55].

The XRD patterns further confirmed the crystalline nature of CuO NPs. Distinct diffraction peaks corresponded well with the monoclinic phase of CuO, affirming phase purity and structural integrity. The nanoscaffold composite, however, displayed a mixed pattern with broader peaks, indicative of a semi-crystalline structure. The reduced crystallinity (20.2%) and broadened peak widths, particularly the full width at half maximum (FWHM) at 43.067°, are typical of polymer-nanoparticle hybrids and point to the nanoscale dispersion of CuO within the matrix. Furthermore, subtle peak shifts imply chemical interactions at the nanoparticle–polymer interface, likely mediated by the phytoconstituents from *G. corticata*. These structural changes provide supportive evidence of uniform nanoparticle integration, which is critical for consistent material performance [56-59].

Morphological analysis through SEM revealed well-formed electrospun nanofibers, exhibiting diameters ranging between 90–150 nm. The absence of bead formation or fiber distortion signifies optimal electrospinning conditions and a homogeneous polymer solution. The CuO NPs, observed as uniformly dispersed spherical entities (<100 nm), were embedded within or attached to the nanofiber surfaces without signs of aggregation. This uniformity highlights the effectiveness of algal metabolites in stabilizing nanoparticles and promoting their compatibility with the polymer matrix. The stable dispersion of nanoparticles within the nanoscaffold is essential for ensuring consistent mechanical and biological properties [60-64].

TGA demonstrated the thermal behavior and stability of the fabricated nanoscaffold. The material underwent two major stages of weight loss, reflecting the decomposition of organic content followed by the degradation of more stable fractions. The high onset temperature (~265°C) and the maximum decomposition near 448°C indicate an enhancement in thermal resistance due to nanoparticle incorporation. Such thermal reinforcement is a hallmark of inorganic–organic composites, where CuO NPs act as thermally stable fillers. Additionally, bioactive compounds from *G. corticata* may act as secondary stabilizers, contributing to delayed thermal degradation by forming protective interactions with the polymer chains [65, 66].

The colloidal properties of the synthesized CuO NPs were further evaluated through DLS and zeta potential analysis. The average particle size of 68.6 nm with a moderate PDI (= 0.584) indicates a reasonably homogeneous distribution. The negative zeta potential value (-14.11 mV) reflects moderate electrostatic repulsion, which is sufficient to prevent immediate aggregation but may benefit from further surface modification for long-term colloidal stability. The biomolecules from *G. corticata* likely contribute to this surface charge through their anionic functional groups, enhancing dispersion stability in aqueous environments [67].

Finally, the anti-inflammatory potential of the extract, CuO NPs, and nanoscaffolds was evaluated using protein denaturation and xanthine oxidase inhibition assays. All samples exhibited concentration-dependent inhibition, with the nanoscaffold consistently outperforming the others. The enhanced bioactivity of the nanoscaffold can be attributed to synergistic effects between CuO NPs and the starch/PVA matrix, which likely improves the bioavailability and activity of the incorporated agents. The reproducibility of the data across replicates and the close approximation of nanoscaffold activity to that of the standard drug (diclofenac sodium) reinforces the material's potential for biomedical application [68].

Overall, these findings demonstrate that *G. corticata*-mediated CuO NPs integrated into electrospun starch/PVA scaffolds offer a promising route for fabricating multifunctional biomaterials. The combined structural, thermal, and biological enhancements highlight the scaffold's potential as a biocompatible, anti-inflammatory platform for future therapeutic applications.

5. CONCLUSION

This study successfully demonstrated the green synthesis of CuO NPs using *G. corticata* extract and their effective incorporation into starch/PVA-based electrospun nanoscaffolds. Characterization techniques, including UV–Vis, FTIR, XRD, SEM, TGA, DLS, and zeta potential analysis, confirmed the structural integrity, stability, and compatibility of the CuO NPs within the nanofibrous matrix. The nanoscaffolds exhibited favorable morphological and thermal properties, with uniform nanoparticle distribution and improved thermal resistance. Notably, anti-inflammatory assays revealed superior inhibition activity by the CuO NP-loaded nanoscaffolds compared to the extract and nanoparticles alone, indicating a synergistic enhancement in biological efficacy. These findings highlight the potential of *G. corticata*-mediated CuO NPs as functional biomaterials for therapeutic applications. The developed nanoscaffolds offer a promising avenue for anti-inflammatory treatments, warranting further *in vivo* studies to establish clinical relevance and potential for biomedical translation.

Ethical Declaration: Not Applicable

Data Availability Statement: The full dataset of physiochemical characterization associated with this work is published in Mendeley Data **[Dataset]** Sustainable nanohybrid systems: Physiochemical properties of *Gracilaria corticota* extract-mediated copper oxide nanoparticle-loaded starch scaffolds (DOI: 10.17632/763h4wwkrj.1). Disclosure: The material characterization data and figures (e.g., UV, SEM, FTIR, XRD, TGA, Zeta Potential and particle sizer) presented here were generated from a common dataset and are being reused across multiple related studies on nanomaterials. All biological analyses and conclusions are original to each manuscript.

Conflicts of Interest: The authors declare no conflicts of interest.

REFERENCES

[1] Natarajan PM, Umapathy VR, Murali A, Swamikannu B. (2022). Computational Simulations of Identified marine-derived Natural Bioactive Compounds As Potential Inhibitors of Oral Cancer. Future Science OA. 2022; 8(3).

[2] Natarajan PM, Umapathy VR. Role of transcriptomics in the study of oral cancer. Frontiers in Oral Health. 2025; 6:1524364.

[3] Vidhyarekha U, Natarajan PM, Bhuminathan S, Sabarinathan J, Suba R, Vijayalakshmi P. Role of artificial intelligence in Oral Cancer. Advances in Public Health. 2024. 2024: 3664408.

[4] Ganesan A, Kumar NG, Natarajan PM, Gauthaman J. Automated classification of elongated styloid processes using deep learning models-an artificial intelligence diagnostics. Frontiers in Oral Health. 2025; 5: 1424840.
[5] Umapathy VR, Natarajan PM, Swamikannu B. Regenerative Strategies in Dentistry: Harnessing Stem Cells, Biomaterials and Bioactive Materials for Tissue Repair. Biomolecules. 2025; 15: 546.
[6] Natarajan PM. Dental Bioinformnatics-Current Scope and Future perspectives. Research Journal of Pharmacy and Technology. 2022;15(5):2351-6.
[7] Ganesan A, Kumar NG, Natarajan PM. Solanum trilobatum leaf extract-derived silver nanoparticles downregulate the PI3K/AKT/mTOR signaling pathway and attenuate oral squamous cell carcinoma cell proliferation. Journal of Herbmed Pharmacology. 2024; 13(2): 300-307.
[8] Daniel Raja FS, Abraham L, Rangasamy K, Saikia K, Rathankumar AK, Mironescu M, Mironescu I, Palanisamy CP, Kanniappan GV. Next-Generation Microbiome Therapeutics: Psychobiotics and Fecal Microbiota Transplants (FMT) for Mental Health Treatment. Frontiers in Cellular and Infection Microbiology. 2026; 16: 1719357.
[9] Dharmaprakash S, Gunasekaran VP, Sivaramakrishnan R, Kanniappan GV, Jayaraman S, Mironescu M, Rajabathar JR, Mironescu ID, Palanisamy CP. Marine macroalgae-mediated ultrasonic-assisted green synthesis of CuO nanoparticles embedded in starch/PVA electrospun nanoscaffolds for in vitro α-amylase and α-glucosidase inhibitory activity. Scientific Reports. 2026.
[10] Surendran N, Chandrasekaran G, Raju MV, Chandrasekaran MK, Ahalliya RM, Palanisamy CP, Kanniappan GV, Arcot R, Alharbi NS, Thiruvengadam M. Anti-inflammatory potential of ethanolic extract of Maranta arundinacea L.: Insights from COX-2 modulation and oxidative stress analysis. South African Journal of Botany. 2026; 195: 142-151.
[11] Pei J, Senthilkumar MV, Hessini K, Subramaniyam S, Sivaramakrishnan R, Kanniappan GV, Jayaraman S, Palanisamy CP. Green fabrication of starch/PVA/CuO nanoscaffolds using marine macroalgae extract for enhanced anti-inflammatory activity. Sustainable Chemistry and Pharmacy. 2026; 51: 102397.
[12] Balasubramanian V, Loganathan L, Muthuswamy K, Viswanathan TM, Raju MV, Chandrasekaran MK, Ahalliya RM, Poorasamy J, Palanisamy CP, Dominic S, Kanniappan GV. Anticancer therapeutic efficacy of PEGylated β-galactosidase from Aspergillus terreus in DMBA-induced breast cancer: Toxicological, molecular and histopathological evaluation in Wistar rats. International Journal of Biological Macromolecules. 2026; 360: 151856.
[13] Jayaraman S, Eswaran A, Rajagopal P, Palanisamy CP, Veerakumar P, Veeraraghavan VP, Sirasanagandla SR. Neuroendocrine-associated epigenetic factors in cellular senescence: mechanisms and therapeutic implications. Biogerontology. 2026; 27(2): 64.
[14] Ponnusamy B, Rajagopal P, Palanisamy CP, Veeraraghavan VP, Jayaraman S. Mechanistic Exploration of the anticancer activity of Justicia adhatoda Plant Leaf Ethanolic Extract against Colon Cancer Cells: An in silico and in vitro Approach. Asian Pacific Journal of Cancer Prevention. 2026; 27(3): 1069-1080.
[15] Pei J, Saran VS, Sivaramakrishnan R, Kanniappan GV, Pandurangan V, Jayaraman S, Dhayalan VK, Mironescu M, Mironescu ID, Palanisamy CP. Ultrasonic-assisted, Sargassum ilicifolium (brown marine macroalgae)-mediated biogenic synthesis of CuO nanoparticles incorporated in starch/PVA electrospun nanoscaffolds: In vitro safety and antioxidant efficacy assessment. Bioorganic Chemistry. 2026; 173: 109679.
[16] Raj MAPA, Subramaniyam S, Kanniappan GV, Jayaraman S, Palanisamy CP. Sustainable fabrication of starch/PVA/CuO electrospun nanoscaffolds from Turbinaria ornata (marine macroalgae) extract: Physicochemical characterization and antidiabetic evaluation. Kuwait Journal of Science. 2026; 53(2): 100545.
[17] Pei J, Ganesh NS, Subramaniyam S, Sivaramakrishnan R, Kanniappan GV, Jayaraman S, Palanisamy CP. Sustainable fabrication of starch/PVA/CuO electrospun nanoscaffolds from Padina tetrastromatica (Brown macroalgae) extract: Physicochemical characterization and antidiabetic assessment. Sustainable Chemistry One World. 2026; 9: 100195.
[18] Sakthiraj A, Sivaramakrishnan R, Subramaniyam S, Kanniappan GV, Pandurangan V, Jayaraman S, Dhayalan VK, Mironescu M, Mironescu ID, Palanisamy CP. Starch/PVA electrospun nanoscaffolds loaded with ultrasonic-assisted green-synthesis of CuO nanoparticles from marine macroalgae (Gracilaria corticata) extract: Cytotoxicity and antioxidant analysis. Chemical Physics Impact. 2026; 12: 101018.
[19] Raju M, Chandrasekaran MK, Loganathan L, Ahalliya RM, Mironescu M, Mironescu ID, Palanisamy CP, Kanniappan GV. Lipid remodeling and ferroptosis in phosphatidylcholine-mediated tumor–stroma crosstalk. Frontiers in Molecular Biosciences. 2026; 13: 1742305.
[20] Kunamalla R, Panagal M, Palanisamy CP. Biogenic synthesis and fabrication of starch/PVA/CuO electrospun nanoscaffolds from Sargassum ilicifolium (brown marine macroalgae) extract for anticancer activity on HT-29 and MCF-7 cancer cells. Biocatalysis and Agricultural Biotechnology. 2026; 72: 103923.
[21] Pei J, Govindaraj H, Sivaramakrishnan R, Kanniappan GV, Pandurangan V, Dhayalan VK, Mironescu M, Mironescu ID, Jayaraman S, Palanisamy PC. Sustainable fabrication of biopolymer-based (starch/PVA) nanoscaffolds loaded with green-synthesized CuO nanoparticles from Sargassum wightii (marine macroalgae): Cytocompatibility and antioxidant activity. Biomaterials Advances. 2026; 182: 214660.

[22] Pei J, Perumal NC, Meng P, Long Q, Palanisamy CP. Extracellular vesicle-based biosensors for Alzheimer's disease: A new frontier in precision diagnostics. Ageing Research Reviews. 2026; 113: 102904.
[23] Shree P, Sivaramakrishnan R, Kanniappan GV, Pandurangan V, Jayaraman S, Dhayalan VK, Mironescu M, Mironescu ID, Palanisamy CP. Antioxidant and biocompatible CuO-starch/PVA nanoscaffolds via ultrasonic green synthesis using Turbinaria conoides (brown marine macroalgae). Medicine in Drug Discovery. 2025; 28: 100238.
[24] Gong J, Lin J, Guan T, Pei J, Palanisamy CP, El-AtyFrom AMA. selenium tolerance to nanoplastic antagonism: Comprehensive characterization of L. casei SNUT1 and its extracellular vesicle–nanoselenium complex. Food Bioscience. 2025; 74: 107749.
[25] Poochi SP, Sundarraj R, Raju MV, Chandrasekaran MK, Ahalliya RM, Palanisamy CP, Kanniappan GV, Kondapavuluri BK, Thiruvengadam M. Harnessing Nature: Computational and Experimental Insights Into *Ipomoea obscura* Metabolites for Bladder Cancer Therapy. Chemistry and Biodiversity. 2025; 0: e00909.
[26] Dugganaboyana GK, Kannankumar MKG, Shivaramakrishna S, Raju MV, Chandrasekaran MK, Ahalliya RM, Panneerselvam N, Palanisamy CP, Kanniappan GV. Phytochemical insights, antioxidant activity and therapeutic potential of Cassia senna against prostate cancer in Wistar albino rats. Discover Applied Sciences. 2025; 7:1206.
[27] Natarajan SR, Krishnamoorthy R, Alshuniaber MA, Gatasheh MK, Rajagopal P, Veeraraghavan VP, Palanisamy CP, Jayaraman S. KDM1A Facilitates Oncogenic Potential in Colorectal Cancer Progression Through the Activation of AXIN/GSK3β/β-Catenin Signaling Pathways: Evidence From Integrated Transcriptomics and In Vitro Studies. The Journal of Gene Medicine. 2025; 27(11): e70053.
[28] Guan T, Gong J, Lin J, Palanisamy CP, Jinjin Pei J, El-Aty AMA. Machine learning-driven multimodal optimization of selenium biotransformation and flavor profiling in fermented apple–Yacon functional beverages. Innovative Food Science & Emerging Technologies. 2025; 105: 104198.
[29] Natarajan SR, Krishnamoorthy R, Alshuniaber MA, Alsulami TS, Gatasheh MK, Rajagopal P, Palanisamy CP, Govindan R, Veeraraghavan VP, Jayaraman S. ABCE1 facilitates tumour progression via aerobic glycolysis and inhibits cell death in human colorectal cancer cells through the p53 signalling pathway. Scientific Reports. 2025; 15: 24674.
[30] Huang Y, Guo H, Liu Y, Jin W, Palanisamy CP, Pei J, Oz F, El-Aty AMA. Effects of Natural Polysaccharides on the Gut Microbiota Related to Human Metabolic Health. Molecular Nutrition & Food Research. 2025; 69:e202400792.
[31] Poornima K, Meenakshi K.C, Manikandan V.R, Shankari G, Prabhu D, Rathi M.A, Palanisamy CP, Balaji R, Gopalakrishnan V.K. Exploring the anticancer potential of Jerantinine A from *Tabernaemontana coronaria* against prostate, breast, and ovarian cancers: A computational approach. *Journal of Complementary and Integrative Medicine*, 2025 22(2): 363–372.
[32] Palanisamy CP, Poompradub S, Sansanaphongpricha K, Jayaraman S, Subramani K. Faridah Sonsudin gGreen synthesis of Nigella sativa-mediated silver nanoparticles for enhanced antibacterial activity and wound healing: Mechanistic insights and biomedical applications. Environmental Nanotechnology, Monitoring & Management. 2025; 24: 101085.
[33] Surendran N, Raju MV, Chandrasekaran MK, Ahalliya RM, Palanisamy CP, Chandrasekaran G, Kanniappan GV. Physicochemical characterization of starch from Maranta arundinacea L.(arrowroot) rhizomes and its inhibition of COX-2: In vivo validation. Bioactive Carbohydrates and Dietary Fibre. 2025; 33: 100465.
[34] Kannappan P, Chandrasekaran MK, Raju MV, Gopalakrishnan S, Dhamodharan P, Ahalliya RM, Palanisamy CP, Raju B, Kanniappan GV. Exploring the anticancer potential of Jerantinine A from Tabernaemontana coronaria against prostate, breast, and ovarian cancers: a computational approach. Journal of Complementary and Integrative Medicine. 2025; 22(02): 363-372.
[35] Pei J, Kumarasamy RV, Jayaraman S, Kanniappan GV, Long Q, Palanisamy CP. Quercetin-functionalized nanomaterials: Innovative therapeutic avenues for Alzheimer's disease management. Ageing Research Reviews. 2025; 104: 102665.
[36] Jayaraman S, Prasad M, Natarajan SR, Krishnamoorthy R, Alshuniaber MA, Gatasheh MK, Veeraraghavan VP, Rajagopal P, Palanisamy CP. Molecular mechanisms underlying the effects of beta-sitosterol on TGF-β1/Nrf2/SIRT1/p53-mediated signaling in the kidney of a high-fat diet and sucrose-induced type-2 diabetic rat. Chemico-Biological Interactions. 2025; 411: 111443.
[37] Huang Y, Guo H, Liu Y, Jin W, Palanisamy CP, Pei J, Oz F, El-Aty AMA. Effects of Natural Polysaccharides on the Gut Microbiota Related to Human Metabolic Health. Molecular Nutrition & Food Research. 2025; e202400792.
[38] Perumal MKK, Renuka RR, Subbiah SK, Natarajan PM. Artificial intelligence-driven clinical decision support systems for early detection and precision therapy in oral cancer: a mini review. Frontiers in Oral Health. 2025; 6: 1592428.
[39] Ramesh E, Ganesan A, Lakshmi KC, Natarajan PM. Artificial intelligence-based diagnosis of oral leukoplakia using deep convolutional neural networks Xception and MobileNet-v2. Frontiers in Oral Health. 2025; 6: 1414524.

[40] Ganesan A, Kumar NG, Natarajan PM. Anticancer activity of silver nanoparticles synthesized from aqueous leaf extract of Solanum trilobatum (Purple fruit pea eggplant) on human oral cancer cells. Journal of Herbmed Pharmacololgy. 2024; 13(2): 260-268.
[41] Natarajan PM, Swamikannu B, Sivaraman NM, Stylin AGSQ. Prevention of Oral Cancer: A Comprehensive Guide. Journal of Pharmacy and Bioallied Sciences. 2024; 16(5): S4239-S4241.
[42] Umapathy V, Dhanavel A, Kesavan R, Natarajan PM, Bhuminathan S, Vijayalakshmi P. Anticancer Potential of the Principal Constituent of Piper nigrum, Piperine: A Comprehensive Review. Cureus. 2024; 16(2): e54425.
[43] Umapathy VR, Swamikannu B, Natarajan PM, Devi R, Nandini MS, Vimalarani, Vijayalakshmi P. In Silico Molecular Docking of Ocimum sanctum Phytochemicals: Targeting Key Biomarkers in Oral Cancer. Journal of Pharmacy and Bioallied Sciences. 2024; 16(5): S4792-S4799.
[44] Natarajan PM, Bhuminathan S, Rajan R, Bindu K, Loganathan K, Veerakumar R. The Crucial Role of Smoking Cessation in Preventing Oral Cancer. Journal of Pharmacy and Bioallied Sciences. 2024; 16(5): S4245-S4247.
[45] Swamikannu B, Umapathy VR, Natarajan PM, Nandini MS, Stylin AGSQ, Vimalarani V, Rajinikanth S. Unlocking the Therapeutic Benefits of Artemisia Annua: A Comprehensive Overview of its Medicinal Properties. Journal of Pharmacy and Bioallied Sciences. 2024; 16(5): S4248-S4253.
[46] Natarajan PM. Computational Studies on Recent Congeners of Fluoroquinolones and Nitroimidazoles for Their Use in Periodontal Therapy. Journal of Pharmacy and Bioallied Sciences. 2024; 16(5): S4731-S4740.
[47] Yadalam PK, Arumuganainar D, Natarajan PM, Ardila CM. Artificial intelligence-powered prediction of AIM-2 inflammasome sequences using transformers and graph attention networks in periodontal inflammation. Scientific Reports. 2025; 15: 8733.
[48] Yadalam PK, Chatterjee S, Natarajan PM, Ardila CM. Comparison of light gradient boosting and logistic r egression for interactomic hub genes in Porphyromonas gingivalis and Fusobacterium nucleatum-induced periodontitis with Alzheimer's disease. Frontiers in Oral Health. 2025; 6:1463458.
[49] Natarajan PM, Bhuminathan S, Leela B, Bindu K, Loganathan K, Ramachandran V. Smoking and its Role in Oral Cancer. Journal of Pharmacy and Bioallied Sciences 16(5): S4242-S4244.
[50] Yadalam PK, Natarajan PM, Ardila CM. Variational graph autoencoder for reconstructed transcriptomic data associated with NLRP3 mediated pyroptosis in periodontitis. Scientific Reports. 2025; 15: 1962.
[51] Prabhakaran P, Palanisamy CP, Shanmugam A, Damodharan P, Swaminathan H, Devaraj D, Ahalliya RM, Kanniappan GV. Isolation, structural characterization, and molecular docking studies on the bioactive compound from n-Hexane extract of Emilia sonchifolia (L.) DC against the pancreatic cancer target Aurora 2 Kinase. Journal of Complementary and Integrative Medicine. 2024; 22(1): 0290.
[52] Jiang H, Kumarasamy RV, Pei J, Raju K, Kanniappan GV, Palanisamy CP. Integrating engineered nanomaterials with extracellular vesicles: Advancing targeted drug delivery and biomedical applications. Frontiers in Nanotechnology. 2024; 6: 1513683.
[53] Guo H, Liu Y, Wan T, Song D, Palanisamy CP, Geng J, Pei J, Özmen S, El-Aty AMA. Toward personalized cancer management: Role of precision nutrition–diet interventions. Journal of Functional Foods. 2024; 123: 106584.
[54] Natarajan SR, Krishnamoorthy R, Alshuniaber MA, Al-Anazi KM, Farah MA, Rajagopal P, Palanisamy CP, Veeraraghavan VP, Jayaraman S. Identification of FOXM1 as a novel protein biomarker and therapeutic target for colorectal cancer progression: Evidence from immune infiltration and bioinformatic analyses. International Journal of Biological Macromolecules. 282 (Part 4): 137201.
[55] Rajendran MS, Jayaraman S, Khan JM, Jasmine S, Prabhakaran RK, Raju MV, Chandrasekaran MK, Ahalliya RM, Kannappan P, Palanisamy CP, Kanniappan GV. Investigating the colon toxicity and carcinogenic role of monosodium glutamate compared with Dimethylhydrazine in male Wistar rats: Exploring the link to childhood colon cancer risk. Journal of King Saud University - Science. 2024; 36(11): 103507.
[56] Kumarasamy RV, Natarajan P, Umapathy VR, Roy JR, Rab SO, Saeed M, Panagal M, Mironescu M, Srinivasan GP, Palanisamy CP. Clinical Applications and Therapeutic Potentials of Advanced Nanoparticles: A Comprehensive Review on Completed Human Clinical Trials. Frontiers in Nanotechnology. 2024; 6:1479993.
[57] Jin W, Pei JJ, Roy JR, Jayaraman S, Ahalliya RM, Kanniappan GV, Mironescu M, Palanisamy CP. Comprehensive review on single-cell RNA sequencing: A new frontier in Alzheimer's disease research. Ageing Research Reviews. 2024; 274: 102454.
[58] Pei J, Palanisamy CP, Jayaraman S, Natarajan PM, Umapathy VR, Roy JR, Panagal M, Jayaraman S. Curcumin-loaded polymeric nanomaterials as a novel therapeutic strategy for Alzheimer's disease: A comprehensive review. Ageing Research Reviews. 2024; 99: 102393.
[59] Pei J, Palanisamy CP, Jayaraman S, Natarajan PM, Umapathy VR, Roy JR, Thalamati D, Ahalliya RM, Kanniappan GV, Mironescu M. A comprehensive review on starch-based Sustainable Edible Films Loaded with Bioactive Components for Food Packaging. International Journal of Biological macromolecules. 2024; 274 (Part-1): 133332.

[60] Palanisamy CP, poompradub S, Sansanaphongpricha K, Subramani K, Sonsudin F. Increased expression levels of PDGF and VEGF magnify the wound healing potential facilitated by biogenic synthesis of silver nanoparticles. Nano-Structures & Nano-Objects. 2024; 39: 101236.
[61] Pei J, Palanisamy CP, Jayaraman S, Natarajan PM, Umapathy VR, Roy JR, Thalamati D, Ahalliya RM, Kanniappan GV, Mironescu M. Proteomics Profiling of Extracellular Vesicle for Identification of Potential Biomarkers in Alzheimer's Disease: A Comprehensive Review. Ageing Research Reviews. 2024; 99: 102359.
[62] Xi J, Wang T, Xian P, Liu X, Du M, Yang H, Palanisamy CP, Lin W, Long Q. Proteomic insights uncover enhanced neurotherapeutic potential in conditioned mesenchymal stem cell-derived extracellular vesicles. Extracellular Vesicle. 2024; 3: 100037.
[63] Pei J, Natarajan PM, Umapathy VR, Swamikannu B, Sivaraman NM, Krishnasamy L, Palanisamy CP. Advancements in the synthesis and functionalization of zinc oxide-based nanomaterials for enhanced oral cancer therapy. Molecules. 2024; 29(11): 2706.
[64] Gatasheh MK, Natarajan SR, Krishnamoorthy R, Alsulami TS, Rajagopal P, Palanisamy CP, Veeraraghavan VP, Jayaraman S. Molecular analysis to identify novel potential biomarkers as drug targets in colorectal cancer therapy: an integrated bioinformatics analysis. Molecular and Cellular Oncology. 2024; 11(1): 2326699.
[65] Pei J, Yan Y, Jayaraman S, Rajagopal P, Natarajan PM, Umapathy VR, Gopathy S, Roy JR, Sadagopan CS, Thalamati D, Palanisamy CP, Mironescu M. A review on advancements in the application of starch-based nanomaterials in biomedicine: Precision drug delivery and cancer therapy. International Journal of Biological Macromolecules. 2024; 130746.
[66] Pei JJ, Yan Y, Palanisamy CP, Jayaraman S, Natarajan PM, Umapathy VR, Gopathy S, Roy JR, Sadagopan JC, Thalamati D, Mironescu M. Materials-based drug delivery approaches: Recent advances and future perspectives. Green Processing and Synthesis. 2024; 13: 20230094.
[67] Pei JJ, Deng W, Liu Y, Guo Y, Chen J, Abdu H, Khan MR, Palanisamy CP, El-Aty AM. A Comprehensive Review of Cornus officinalis: Health Benefits, Phytochemistry, and Pharmacological Effects for Functional Drug and Food Development. Frontiers in Nutrition. 2023; 10: 1309963.
[68] Lavanya M, Krishnamoorthy R, Alshuniaber MA, Manoharadas S, Palanisamy CP, Veeraraghavan VP, Jayaraman S, Rajagopal P, Padmini R. Formulation, characterization and evaluation of gelatin-syringic acid/zinc oxide nanocomposite for its effective anticancer, antioxidant and anti-inflammatory activities. Journal of King Saud University-Science. 2023; 35: 102909.